Analytical Methods

PAPER

View Article Online
View Journal | View Issue

Cite this: *Anal. Methods*, 2019, **11**, 157

Electrochemical determination of PIK3CA gene associated with breast cancer based on molybdenum disulfide nanosheet-supported poly(indole-6-carboxylic acid)†

Jimin Yang,‡ Xuesong Yin‡ and Wei Zhang *

Received 7th November 2018
Accepted 23rd November 2018

DOI: 10.1039/c8ay02425a

rsc.li/methods

In our study, we report the development of molybdenum disulfide (MoS_2) nanosheet-supported poly(indole-6-carboxylic acid) (PIn6COOH) and its usage for the electrochemical determination of circulating tumor DNA (ctDNA) such as PIK3CA gene associated with breast cancer. The MoS_2 nanosheets prepared by the solvent exfoliation method from commercial bulk MoS_2 were first immobilized on the surface of a carbon paste electrode; then, PIn6COOH, a novel electroactive material, was electropolymerized on the MoS_2 substrate by the potentiostatic method to form a unique nanocomposite structure. The physical adsorption between aromatic In6COOH monomers and MoS_2 efficiently improved the electropolymerization efficiency, resulting in increased electrochemical response of PIn6COOH. Owing to the presence of abundant carboxyl groups, probe ssDNA was covalently immobilized on the carboxyl-terminated PIn6COOH/MoS_2 nanocomposite through free amines of DNA sequences based on 1-ethyl-3-(3-dimethylaminopropyl)carbodiimide and *N*-hydrosulfosuccinimide crosslinking reaction. The covalently immobilized probe ssDNA could selectively hybridize with its target DNA to form dsDNA on the surface of the PIn6COOH/MoS_2 nanocomposite. The self-signal changes of PIn6COOH induced by DNA immobilization and hybridization could be sensitively recognized *via* cyclic voltammetry and electrochemical impedance spectroscopy. This developed biosensor showed high performance of DNA hybridization with a detection limit of 1.5×10^{-17} mol L^{-1} for the detection of PIK3CA gene. The easy construction of this biosensor besides its fine sensitivity and very low time consumption can make this PIn6COOH/MoS_2 nanocomposite very highly competitive for further applications in carcinoma diagnostic and therapeutic fields.

1. Introduction

Circulating tumor DNA (ctDNA) is the fraction of total cell-free DNA fragments circulating in the bloodstream that is derived from cancer cells. Detection of cancer aberrations using relatively noninvasive blood draws is an attractive alternative to tissue biopsies or bone marrow aspirates. By avoiding the pain and complications associated with primary tumor sampling, ctDNA assays enable more frequent testing of patients, thus enabling proactive disease management, detection of early relapse, and longitudinal tracking of minimal residual disease following successful treatment. Due to these unique properties, ctDNA assays in blood can serve as an effective tool for liquid biopsy, potentially replacing other biomarkers in certain diagnostic applications.[1–3] However, although ctDNA is a promising potential biomarker for noninvasive cancer assessment, the detection of mutated ctDNA in serum samples of cancer patients is very challenging because very low amount of ctDNA is present along with abundant wide-type DNA of remarkably higher levels. Therefore, for successful detection of mutated ctDNA, a method must be highly sensitive and selective for detecting the extremely low concentration of mutated ctDNA in the presence of high background levels of unmutated sequences in patient samples. Traditional ctDNA analysis approaches can be broadly divided into amplification and sequencing-based methods. Although the amplification and sequencing-based methods have greatly promoted the development of ctDNA detection, they cannot be applied as a routine diagnostic tool because of many obstacles: they are time-consuming and require extremely high costs and complicated operations.[4] Therefore, developing novel strategies to achieve highly sensitive, specific, cost-effective, and rapid detection of tumor-specific mutations is in urgent demand. For example, Zhou *et al.* reported the detection of ctDNA *via* DNA-mediated surface-

School of Chemistry and Chemical Engineering, Linyi University, Linyi 276005, China. E-mail: zhangweiqust@126.com; Fax: +86-539-7258620; Tel: +86-539-7258620

† Electronic supplementary information (ESI) available. See DOI: 10.1039/c8ay02425a

‡ These two authors contributed equally to this work.

enhanced Raman spectroscopy of single-walled carbon nanotubes.[5] Chu *et al.* reported highly sensitive electrochemical detection of ctDNA based on thin-layer MoS_2/graphene composites.[6]

To obtain better analytical performance, some traditional nanomaterials such as metal nanomaterials and carbon nanomaterials have been introduced to improve the sensitivity of electrochemical sensors due to their large specific surface area, fast electron transfer rates, and abundant bonding sites.[7–13] Two-dimensional (2D) molybdenum disulfide (MoS_2), a layered semiconductor material made of covalently bound S–Mo–S layers stacked through weak van der Waals interactions, is an emerging but important class of inorganic graphene analogs; it has attracted extensive interest due to its predominant properties including high specific surface area, excellent electrochemical catalyst activity, easy functionalization, and remarkable biocompatibility.[14–16] Therefore, 2D MoS_2 is a promising building block for constructing electrochemical sensors.[17–23] For example, Qiao *et al.* constructed a novel electrochemical sensing platform for ultrasensitive detection of cardiac troponin I based on aptamer-MoS_2 nanoconjugates.[17] Dou *et al.* developed a trimetallic hybrid nanoflower-decorated MoS_2 nanosheet sensor for direct *in situ* monitoring of H_2O_2 secreted from live cancer cells.[18] Chand *et al.* reported the synthesis of MoS_2 nanosheets decorated with a copper ferrite nanoparticle composite and molecular probe-immobilized MoS_2 nanosheets as nanocarriers for the electrochemical detection of miRNAs.[19]

Conducting polymers (CPs) or the composites of CPs with nanomaterials have been successfully employed in DNA electrochemical biosensors.[24,25] For DNA electrochemical sensors based on CPs, the polymer is not only used as an immobilization carrier but also plays an active role in signal transduction in the presence of a target-analyzed molecule. As an unconventional CP, poly(indole-6-carboxylic acid) (PIn6COOH) is of much interest due to its several advantages, especially high redox activity and fine stability; it has been used for determination of biomolecules.[26,27] In this study, we report, for the first time, an innovative design of a high-performance biosensing platform for indicator-free electrochemical determination of the PIK3CA gene by employing electropolymerized PIn6COOH on the pre-obtained MoS_2 nanosheet substrate. The PIK3CA gene existing in the peripheral blood of breast cancer patients is a type of ctDNA.[28] The immobilization of probe DNA was successfully accomplished *via* covalent bonding between the abundant carboxyl groups of PIn6COOH/MoS_2 nanocomposite and the free amino groups at the 5′-end of the probe DNA, which caused a "signal-off" model with decreased current response. After the hybridization of probe DNA with target DNA, the formation of double-helix structure induced "signal-on" of the nanocomposite. The conformational and concomitant conductivity changes in the DNA/PIn6COOH/MoS_2 film induced a distinct change in the self-redox signals of the PIn6COOH layer. Cyclic voltammetry (CV) and electrochemical impedance spectroscopy (EIS) were utilized to explore the mechanism of the indicator-free direct electrochemical determination of DNA hybridization.

2. Materials and methods

2.1. Apparatus and materials

Electrochemical measurements were performed on a CHI660E electrochemical analyzer (Shanghai CH Instrument Company, China) with a standard three-electrode configuration. A platinum wire was used as the counter electrode, a saturated calomel electrode (SCE) acted as the reference electrode, and a modified carbon paste electrode (CPE, 3 mm in diameter) was used as the working electrode. Transmission electron microscopy (TEM) was conducted on a JEM-2100 machine (JEOL, Japan).

Indole-6-carboxylic acid (In6COOH, 99%) was ordered from Shanghai Aladdin Biological Technology Corporation (China). Graphite powder (spectral pure, diameter about 30 μm) was obtained from Shanghai Colloid Chemical Plant (China). MoS_2 was acquired from Tianjin Kemiou Chemical Reagent Corporation (China). 1-Ethyl-3-(3-dimethylaminopropyl)carbodiimide (EDC) and *N*-hydrosulfosuccinimide (NHS) were obtained from Sigma-Aldrich (USA). Acetonitrile and *N*,*N*-dimethylformamide (DMF) were purchased from Shanghai Reagent Company (China). All the chemicals were of analytical grade and used without further treatment.

All DNA sequences were synthesized by Shanghai Sangon Biotechnology Limited Company (China), and their base sequences were as follows:

Probe DNA (ssDNA): 5′-NH_2-AGT GAT TTT AGA GAG-3′;

Target DNA (cDNA): 5′-CTC TCT AAA ATC ACT-3′;

Single-base mismatched DNA: 5′-CTC TCT AAA GTC ACT-3′;

Three-base mismatched DNA: 5′-CTA TCT ACA ATG ACT-3′;

Non-complementary DNA (ncDNA): 5′-ATG TCG AGC GTA GCT-3′.

2.2. Fabrication of the sensing interfaces

The exfoliated MoS_2 nanosheets were first prepared by ultrasonicating 10 mg MoS_2 powder in 10 mL DMF for 10 h; then, a homogenous suspension was obtained with the concentration of 1.0 mg mL^{-1}.[29] CPE was fabricated as reported previously.[30] To obtain a smooth surface, the surface of CPE was pre-treated by polishing with a weighing paper. Ten μL of the suspension was uniformly cast on the pre-treated surface of CPE and dried at ambient temperature to obtain MoS_2/CPE.

The prepared electrode (MoS_2/CPE) was subjected to electropolymerization in acetonitrile containing 0.05 mol L^{-1} In6COOH monomer at a fixed potential of 1.4 V for 500 s, and the obtained electrode was denoted as PIn6COOH/MoS_2/CPE. For comparison, the same procedure was employed to fabricate the electrode without MoS_2 nanosheets and was named as PIn6COOH/CPE.

2.3. Immobilization and hybridization of DNA

The ssDNA probes were covalently immobilized on the PIn6COOH/MoS_2/CPE surface through the free amines of the DNA probes using the EDC/NHS cross-linking reaction. The terminal carboxyl groups of the PIn6COOH/MoS_2 nanocomposite were activated by immersion in 0.3 mol L^{-1} PBS (pH 7.0) containing

2.0 mmol L^{-1} EDC and 5.0 mmol L^{-1} NHS for 1 h. The linker/PIn6COOH/MoS_2/CPE was rinsed with PBS (pH 7.0) to wash off the redundant EDC and NHS. Ten μL of PBS (pH 7.0) containing ssDNA probes (1.0×10^{-11} mol L^{-1}) was then dropped onto the chemically modified electrode and air-dried and washed using blank PBS buffer to remove the unbound capture probe; this probe-captured electrode was denoted as ssDNA/PIn6COOH/MoS_2/CPE.

Next, the probe-captured electrode was immersed in hybridization buffer solution (PBS, pH 7.0) containing cDNA (1.0×10^{-11} mol L^{-1}) for 2 h to capture cDNA onto the electrode *via* DNA hybridization, followed by thoroughly washing with blank PBS buffer to remove the unhybridized cDNA. The same procedures as mentioned above were applied to the probe-modified electrode for hybridization with single-base mismatched DNA (1.0×10^{-11} mol L^{-1}), three-base mismatched DNA (1.0×10^{-11} mol L^{-1}) and ncDNA (1.0×10^{-11} mol L^{-1}).

A schematic illustration of the detection process and principle of the self-signal electrochemical sensing platform is displayed in Scheme S1 in the ESI.†

2.4. Electrochemical measurements

The CV experiments were conducted in 0.3 mol L^{-1} PBS (pH 7.0) between the potential window 0.5 V and −0.3 V with a scan rate of 100 mV s^{-1}. The EIS measurements were carried out in 0.3 mol L^{-1} PBS (pH 7.0) in a frequency range from 1 Hz to 10^5 Hz with AC voltage amplitude of 5 mV.

Throughout the experiments, the solution was continuously bubbled with nitrogen to remove any oxygen. Unless specifically noted, all experiments were performed at room temperature.

3. Results and discussion

3.1. TEM characterization

Fig. 1A illustrates the TEM image of the as-prepared MoS_2 nanosheets. From the image, it is clearly seen that layer structures of the MoS_2 nanosheets were successfully prepared, which overlapped with each other and were stacked on the electrode surface. The MoS_2 nanosheets were exfoliated from MoS_2 powder through sonication. The PIn6COOH film formed on bare CPE electropolymerized without MoS_2 displayed a rough surface with many wrinkles, as displayed in Fig. 1B. As shown in Fig. 1C, the resulting PIn6COOH/MoS_2 nanocomposite still comprised stacked nanosheets, but the nanosheets revealed unsmooth surfaces, suggesting that the PIn6COOH agglomerates were formed on the basal surface of MoS_2, due to which the surface became coarse. The results also show that MoS_2 served as a support material and provided a large quantity of active sites for the growth of PIn6COOH.

3.2. Electrochemical behavior of different modified electrodes

As displayed in Fig. 2, the electrochemical behaviors of different modified electrodes were investigated in 0.3 mol L^{-1} PBS (pH 7.0) by monitoring the self-redox signals of PIn6COOH. No CV peaks were observed for bare CPE (curve a). As shown in curve b, the CV response of PIn6COOH/CPE comprised a clear pair of redox peaks, which could be ascribed to the self-redox reactions of the electroactive PIn6COOH film formed on the electrode surface. Compared with the result for PIn6COOH/CPE (curve b), the CV response of PIn6COOH/MoS_2/CPE (curve c) showed

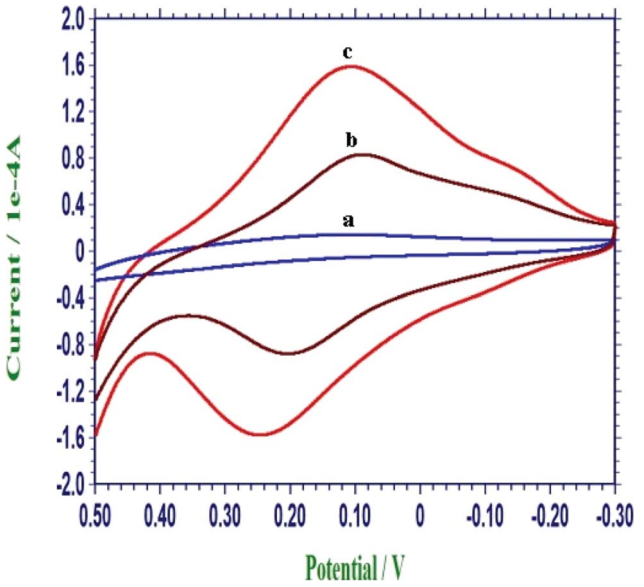

Fig. 2 Representative CVs of bare CPE (a), PIn6COOH/CPE (b) and PIn6COOH/MoS_2/CPE (c) recorded in 0.3 mol L^{-1} PBS (pH 7.0).

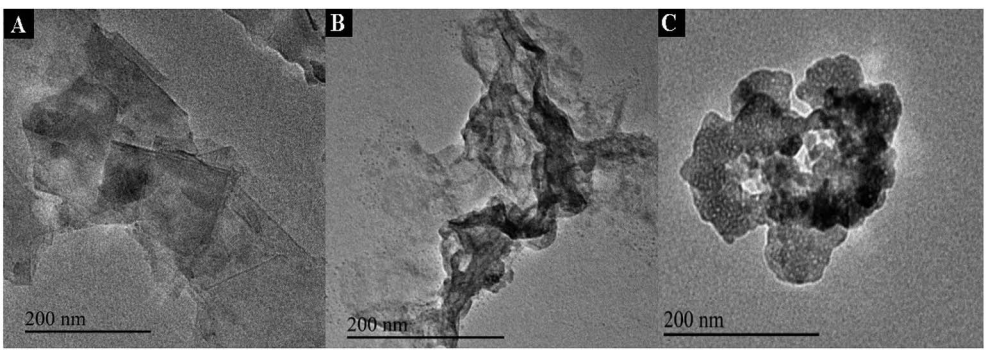

Fig. 1 TEM images of MoS_2 (A), PIn6COOH (B) and PIn6COOH/MoS_2 (C).

a much larger value, which may be due to the following reasons: the MoS_2 nanosheet layer with a large specific surface provided an excellent adsorption platform for In6COOH monomers, which dramatically improved the electropolymerization efficiency and resulted in an increased electrochemical response of PIn6COOH.

3.3. Optimization of the electropolymerization of PIn6COOH

The amount of MoS_2 nanosheets has a major influence on the electropolymerization of PIn6COOH. The electrochemical response of the PIn6COOH/MoS_2 nanocomposite increased gradually with increasing amount of MoS_2 nanosheets, and the maximum response was acquired at 10 μL of 1.0 mg mL^{-1} MoS_2 nanosheets. Low concentration of MoS_2 nanosheets resulted in very thin MoS_2 films; thereby, few binding sites of thin MoS_2 film with In6COOH monomers resulted in weak physical adsorption between MoS_2 and In6COOH. However, when the concentration of MoS_2 nanosheets was larger than 1.0 mg mL^{-1}, a decreased electrochemical response was observed. This might be ascribed to the overlay of the electrode surface by extremely thick layers of MoS_2, which can stack together and prevent effective adsorption and electropolymerization of PIn6COOH. Therefore, 10 μL of 1.0 mg mL^{-1} MoS_2 nanosheets was used for electrode modification in our experiments.

The electrochemical properties of the PIn6COOH/MoS_2 nanocomposite appeared to be affected by the electrochemical preparation parameters, especially the electropolymerization time. In the experiments, the polymerization potential was maintained at an invariable potential of 1.4 V. The self-redox response of PIn6COOH was employed as the indicator to optimize the electropolymerization time. The electrochemical signals of the PIn6COOH/MoS_2 nanocomposite increased as the electropolymerization time increased and reached the maximum at 500 s; then, the signal decreased with further electropolymerization. Accordingly, the time of 500 s was chosen as the electropolymerization time.

3.4. Self-signal monitoring of DNA immobilization and hybridization

As displayed in Fig. 3, the electrochemical self-signals of PIn6COOH/MoS_2/CPE after DNA immobilization and hybridization were investigated using CV in 0.3 mol L^{-1} PBS (pH 7.0). As mentioned above, the resulting PIn6COOH/MoS_2/CPE demonstrated favorable electrochemical activities in a neutral environment (curve a). After the amino-functionalized probe ssDNA was immobilized on the surface of PIn6COOH/MoS_2 nanocomposite with abundant carboxyl groups by covalent bonding, the self-redox response of ssDNA/PIn6COOH/MoS_2/CPE decreased drastically (curve b). The probe ssDNA behaves as random coils and possesses flexible traits, which may change the conformation and block effective electron transfer along the PIn6COOH chains;[31] this resulted in decreased response of the ssDNA/PIn6COOH/MoS_2 layer ("signal-off"). However, after hybridization of the probe ssDNA with cDNA, an increase in the CV response (curve c, "signal-on") was observed compared with

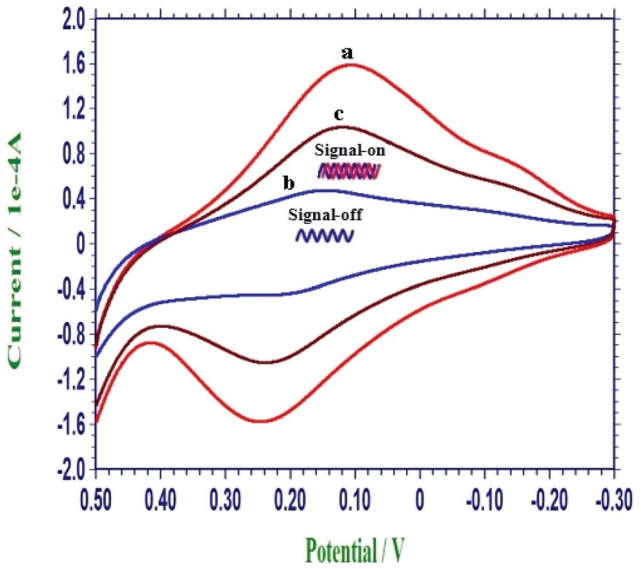

Fig. 3 Representative CVs of PIn6COOH/MoS_2/CPE (a), ssDNA/PIn6COOH/MoS_2/CPE (b) and dsDNA/PIn6COOH/MoS_2/CPE (c) recorded in 0.3 mol L^{-1} PBS (pH 7.0).

that observed in curve b. Current enhancement upon hybridization may be due to changes in the conformation of DNA. Indeed, ssDNA behaves as random coils, whereas dsDNA leads to a more organized surface, through which counter ions along the double-helix structure can diffuse more freely. At the same time, ssDNA is a flexible molecule, whereas dsDNA acts as a rigid rod; therefore, the electron transfer rate along the double-helix structure is much faster than that along the single-chain structure.[32,33] Consequently, the self-redox signals increase ("signal-on") after the ssDNA probes hybridize with cDNA. The above results reveal that the self-redox signal changes of the PIn6COOH layer can be employed as a simple and effective tool for direct DNA determination by CV without the requirement of any external indicators and addition of any labels to the DNA probes or target molecules.

3.5. Specificity of the developed DNA biosensor

To evaluate the specificity of the developed biosensor, some different nonspecific interference DNA sequences including target DNA, single-base mismatched DNA, three-base mismatched DNA and ncDNA were tested in 0.3 mol L^{-1} PBS (pH 7.0), and the results are shown in Fig. 4. Curve a represents the Bode plot of PIn6COOH/MoS_2/CPE. As seen in curve f, when the probe ssDNA was covalently bound to the PIn6COOH/MoS_2 nanocomposite, the impedance response increased, evidently indicating successful immobilization of the probe ssDNA. After hybridization with the target DNA, a remarkable decrease in the impedance was observed (curve b). The EIS results were consistent with the above CV results. The impedances related to the single-base mismatched DNA (curve c) and three-base mismatched DNA (curve d) were larger than that observed for curve b, illustrating that complete hybridization was not realized owing to base mismatch. As displayed in curve e, when hybridized with ncDNA, the impedance response varied

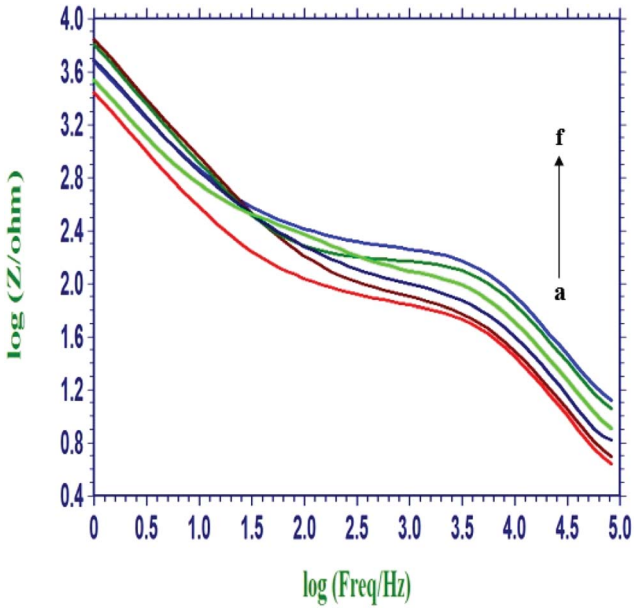

Fig. 4 Representative Bode plots recorded for PIn6COOH/MoS_2/CPE (a), ssDNA/PIn6COOH/MoS_2/CPE (f), dsDNA/PIn6COOH/MoS_2/CPE (hybridized with cDNA, (b)), hybridized with single-base mismatched DNA (c), hybridized with three-base mismatched DNA (d), and hybridized with ncDNA (e) in 0.3 mol L^{-1} PBS (pH 7.0).

negligibly compared with that observed for curve f, indicating that nearly no hybridization occurred. These results demonstrate the high specificity of the constructed indicator-free DNA biosensor based on PIn6COOH/MoS_2 nanocomposite to its complementary target DNA.

3.6. Analytical performance of the biosensor

Under optimal experimental conditions, the proposed probe ssDNA/PIn6COOH/MoS_2/CPE was incubated with a series of concentrations of target DNA, and the obtained Bode plots are shown in Fig. 5A. The impedance decreased as the target DNA concentrations increased from 1.0×10^{-16} mol L^{-1} to 1.0×10^{-11} mol L^{-1}. The difference ($\Delta\log Z$) between the log Z values (at a frequency range of 10^5 Hz) of the probe-modified electrode before and after hybridization with cDNA was used as the measurement signal. Fig. 5B shows linear dependence between the $\Delta\log Z$ value and the logarithm of the target sequence concentrations with the linear regression equation $\Delta\log Z = 0.0691 \log C + 1.2134$ and regression coefficient (R) of 0.9968. The detection limit was calculated to be 1.5×10^{-17} mol L^{-1} (based on S/N = 3). The performance of the developed biosensor was compared with those of some other DNA electrochemical biosensors based on poly(indole-6-carboxylic acid), as shown in Table 1. The results show that this proposed DNA biosensor possesses a remarkable detection limit and wide detection range for target DNA recognition.

3.7. Stability and reproducibility of the DNA biosensor

The stability of the developed DNA biosensor was investigated. The prepared DNA biosensor was stored in PBS (pH 7.0) under the same conditions at 4 °C for three weeks and then, the

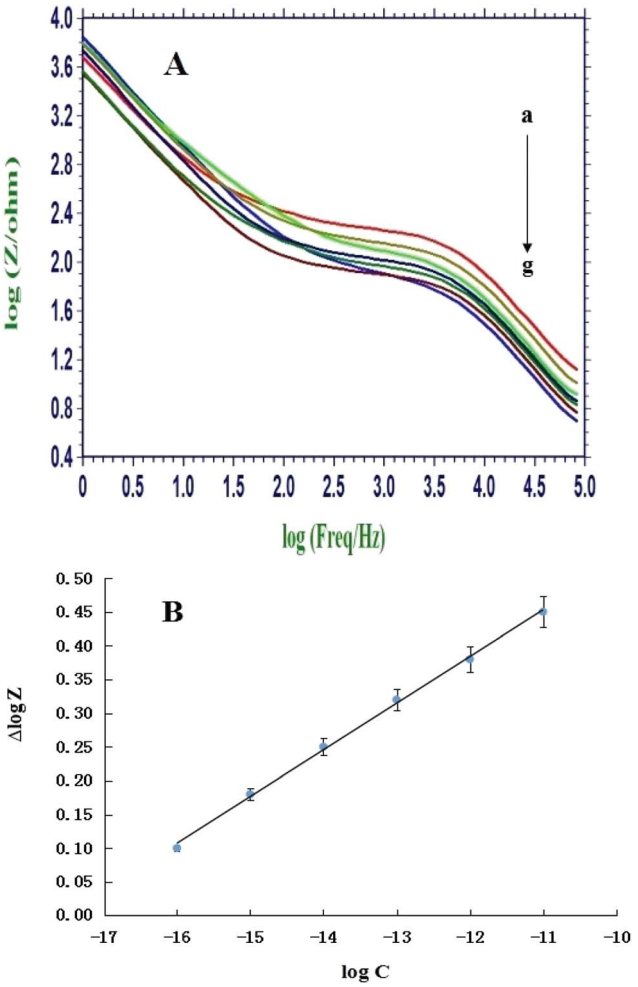

Fig. 5 (A) Representative Bode plots recorded for the ssDNA/PIn6-COOH/MoS_2/CPE (a) and after hybridization reaction with different concentrations of PIK3CA gene target sequences: (b) 1.0×10^{-16}, (c) 1.0×10^{-15}, (d) 1.0×10^{-14}, (e) 1.0×10^{-13}, (f) 1.0×10^{-12} and (g) 1.0×10^{-11} mol L^{-1} in 0.3 mol L^{-1} PBS (pH 7.0). (B) The plot of $\Delta\log Z$ *versus* the logarithm of the PIK3CA gene target sequence concentrations.

impedance response was recorded. The signal still remained at 93.8% compared with the initial value, indicating that the biosensor exhibited good stability within three weeks.

The reproducibility of the DNA hybridization recognition platform is also particularly significant in the DNA analysis. Six parallel-prepared probe electrodes were used to detect 1.0×10^{-16} mol L^{-1} target DNA sequences with a relative standard deviation of 5.33%, implying that the proposed biosensor has acceptable reproducibility for the detection of target DNA.

4. Conclusions

In summary, a highly sensitive electrochemical strategy for convenient detection of PIK3CA gene related to breast cancer was developed for the first time. Sensitive detection was attained by using PIn6COOH-functionalized MoS_2 nanosheets as the signal-transduction material. The proposed biosensor exhibited a low detection limit, wide linear range, high

Table 1 Comparison of the performance of the developed biosensor with that of some other DNA electrochemical biosensors based on poly(indole-6-carboxylic acid)

	This work	Ref. 34	Ref. 27
Electrodes	Poly(indole-6-carboxylic acid)/MoS_2/CPE	Poly(indole-6-carboxylic acid)/GCE	Poly(indole-6-carboxylic acid)-MWNT/GCE
Detection methods	EIS (PBS)	CV (NaAc-HAc)	CV (NaAc-HAc)
Detection limit (mol L^{-1})	1.5×10^{-17}	5.79×10^{-12}	2.0×10^{-15}
Detection range (mol L^{-1})	1.0×10^{-16} to 1.0×10^{-11}	3.5×10^{-10} to 2.0×10^{-8}	1.0×10^{-14} to 5.0×10^{-12}

specificity, good stability and excellent reproducibility. We believe that the designed biosensor can serve as a promising candidate for sensitive detection of DNA in biological samples and may be used for applications in the early clinical diagnosis and therapy of breast cancer.

Conflicts of interest

There are no conflicts to declare.

Acknowledgements

This work was supported by the Natural Science Foundation of Shandong Province (No. ZR2017QB013), the Undergraduate Training Program for Innovation and Entrepreneurship of Linyi University (No. 201810452170), and the Undergraduate Teaching Reform Project of Shandong Province (No. Z2018S006).

References

1 T. J. Pugh, *Semin. Hematol.*, 2018, **55**, 38–40.
2 A. E. Rodda, B. J. Parker, A. Spencer and S. R. Corrie, *ACS Sens.*, 2018, **3**, 540–560.
3 L. Lu, J. Q. Bi and L. M. Bao, *J. Genet. Genomics*, 2018, **45**, 79–85.
4 P. Hu, S. J. Zhang, T. Wu, D. L. Ni, W. P. Fan, Y. Zhu, R. Qian and J. L. Shi, *Adv. Mater.*, 2018, **30**, 1801690.
5 Q. F. Zhou, J. Zheng, Z. H. Qing, M. J. Zheng, J. F. Yang, S. Yang, L. Ying and R. H. Yang, *Anal. Chem.*, 2016, **88**, 4759–4765.
6 Y. L. Chu, B. Cai, Y. Ma, M. G. Zhao, Z. Z. Ye and J. Y. Huang, *RSC Adv.*, 2016, **6**, 22673–22678.
7 R. Y. Zhang, Y. Zhang, X. L. Deng, S. G. Sun and Y. C. Li, *Electrochim. Acta*, 2018, **271**, 417–424.
8 Y. Zhao, Y. X. Yang, L. Y. Cui, F. J. Zheng and Q. J. Song, *Biosens. Bioelectron.*, 2018, **117**, 53–59.
9 K. Shim, J. Kim, M. Shahabuddin, Y. Yamauchi, M. S. A. Hossain and J. H. Kim, *Sens. Actuators, B*, 2018, **255**, 2800–2808.
10 S. M. Yu, H. F. Li, G. G. Li, L. T. Niu, W. L. Liu and X. Di, *Talanta*, 2018, **184**, 244–250.
11 M. A. Mohamed, D. M. El-Gendy, N. Ahmed, C. E. Banks and N. K. Allam, *Biosens. Bioelectron.*, 2018, **101**, 90–95.
12 S. A. Zaidi, *Electrochim. Acta*, 2018, **274**, 370–377.
13 Z. Z. Yin, S. W. Cheng, L. B. Xu, H. Y. Liu, K. Huang, L. Li, Y. Y. Zhai, Y. B. Zeng, H. Q. Liu, Y. Shao, Z. L. Zhang and Y. X. Lu, *Biosens. Bioelectron.*, 2018, **100**, 565–570.
14 A. Sinha, Dhanjai, B. Tan, Y. J. Huang, H. M. Zhao, X. M. Dang, J. P. Chen and R. Jain, *Trends Anal. Chem.*, 2018, **102**, 75–90.
15 S. Barua, H. S. Dutta, S. Gogoi, R. Devi and R. Khan, *ACS Appl. Nano Mater.*, 2018, **1**, 2–25.
16 Z. H. Hu, Z. T. Wu, C. Han, J. He, Z. H. Ni and W. Chen, *Chem. Soc. Rev.*, 2018, **47**, 3100–3128.
17 X. J. Qiao, K. X. Li, J. Q. Xu, N. Cheng, Q. L. Sheng, W. Cao, T. L. Yue and J. B. Zheng, *Biosens. Bioelectron.*, 2018, **113**, 142–147.
18 B. T. Dou, J. M. Yang, R. Yuan and Y. Xiang, *Anal. Chem.*, 2018, **90**, 5945–5950.
19 R. Chand, S. Ramalingam and S. Neethirajan, *Nanoscale*, 2018, **10**, 8217–8225.
20 R. Aswathi and K. Y. Sandhya, *J. Mater. Chem. A*, 2018, **6**, 14602–14613.
21 W. Zhang, Z. C. Dai, X. Liu and J. M. Yang, *Biosens. Bioelectron.*, 2018, **105**, 116–120.
22 D. P. Li, X. Y. Liu, R. Yi, J. X. Zhang, Z. Q. Su and G. Wei, *Inorg. Chem. Front.*, 2018, **5**, 112–119.
23 X. R. Gan, H. M. Zhao, K. Y. Wong, D. Y. Lei, Y. B. Zhang and X. Quan, *Talanta*, 2018, **182**, 38–48.
24 T. Yang, L. Meng, J. L. Zhao, X. X. Wang and K. Jiao, *ACS Appl. Mater. Interfaces*, 2014, **6**, 19050–19056.
25 W. Zhang, Q. T. Hu, Y. C. Su and X. W. Zheng, *J. Electroanal. Chem.*, 2014, **719**, 72–76.
26 P. C. Pandey, D. S. Chauhan and V. Singh, *Electrochim. Acta*, 2009, **54**, 2266–2270.
27 G. M. Nie, Z. M. Bai, J. Chen and W. Y. Yu, *ACS Macro Lett.*, 2012, **1**, 1304–1307.
28 H. Schneck, C. Blassl, F. Meier-Stiegen, R. P. Neves, W. Janni, T. Fehm and H. Neubauer, *Mol. Oncol.*, 2013, **7**, 976–986.
29 F. Chekin, F. Teodorescu, Y. Coffinier, G. H. Pan, A. Barras, R. Boukherroub and S. Szunerits, *Biosens. Bioelectron.*, 2016, **85**, 807–813.
30 W. Zhang, T. Yang, X. Li, D. B. Wang and K. Jiao, *Biosens. Bioelectron.*, 2009, **25**, 428–434.
31 Y. W. Hu, T. Yang, X. X. Wang and K. Jiao, *Chem.–Eur. J.*, 2010, **16**, 1992–1999.
32 M. C. Pham, B. Piro and L. D. Tran, *Anal. Chem.*, 2003, **75**, 6748–6752.
33 Q. D. Zhang, B. Piro, V. Noel, S. Reisberg and M. C. Pham, *Analyst*, 2011, **136**, 1023–1028.
34 G. M. Nie, Y. Zhang, Q. F. Guo and S. S. Zhang, *Sens. Actuators, B*, 2009, **139**, 592–597.

